Molecular Therapy
Nucleic Acids
Original Article

A humanized knockin mouse model of Duchenne muscular dystrophy and its correction by CRISPR-Cas9 therapeutic gene editing

Yu Zhang,[1,2] Hui Li,[1,2] Takahiko Nishiyama,[1,2] John R. McAnally,[1,2] Efrain Sanchez-Ortiz,[1,2] Jian Huang,[3] Pradeep P.A. Mammen,[2,3] Rhonda Bassel-Duby,[1,2] and Eric N. Olson[1,2]

[1]Department of Molecular Biology, University of Texas Southwestern Medical Center, Dallas, TX 75390, USA; [2]Senator Paul D. Wellstone Muscular Dystrophy Specialized Research Center, University of Texas Southwestern Medical Center, Dallas, TX 75390, USA; [3]Department of Internal Medicine, University of Texas Southwestern Medical Center, Dallas, TX 75390, USA

Duchenne muscular dystrophy (DMD) is a lethal neuromuscular disease caused by mutations in the X-linked dystrophin (*DMD*) gene. Exon deletions flanking exon 51, which disrupt the dystrophin open reading frame (ORF), represent one of the most common types of human DMD mutations. Previously, we used clustered regularly interspaced short palindromic repeats (CRISPR) and CRISPR-associated proteins (Cas) gene editing to restore the reading frame of exon 51 in mice and dogs with exon 50 deletions. Due to genomic sequence variations between species, the single guide RNAs (sgRNAs) used for DMD gene editing are often not conserved, impeding direct clinical translation of CRISPR-Cas therapeutic gene-editing strategies. To circumvent this potential obstacle, we generated a humanized DMD mouse model by replacing mouse exon 51 with human exon 51, followed by deletion of mouse exon 50, which disrupted the dystrophin ORF. Systemic CRISPR-Cas9 gene editing using an sgRNA that targets human exon 51 efficiently restored dystrophin expression and ameliorated pathologic hallmarks of DMD, including histopathology and grip strength in this mouse model. This unique DMD mouse model with the human genomic sequence allows *in vivo* assessment of clinically relevant gene editing strategies as well as other therapeutic approaches and represents a significant step toward therapeutic translation of CRISPR-Cas9 gene editing for correction of DMD.

INTRODUCTION

Skeletal muscle is indispensable for a variety of human activities. Despite the remarkable regeneration capacity of skeletal muscle, it is vulnerable to numerous pathological disorders, including myopathies and muscular dystrophies. Among them, Duchenne muscular dystrophy (DMD) represents one of the most devastating muscle disorders. DMD is a progressive muscle disease, caused by mutations in the *DMD* gene located on the X chromosome.[1,2] The protein product of the *DMD* gene is dystrophin, a large intracellular protein essential for tethering the inner cytoskeleton and extracellular matrix.[3] Loss of dystrophin protein in skeletal muscle and the heart causes membrane leakage during muscle contraction, leading to contraction-induced damage, followed by muscle fibrosis, cardiomyopathy, respiratory failure, and, ultimately, premature death.[4] Despite extensive efforts, DMD remains the leading cause of early death in boys affected with monogenic muscle disorders, highlighting the need for effective therapies.

In contrast to conventional gene replacement therapy, gene editing therapy uses a programmable nuclease to correct disease-causing mutations at the genome level. Among the different programmable nucleases developed so far, clustered regularly interspaced short palindromic repeats (CRISPR) and CRISPR-associated proteins (Cas) offer simplicity and accuracy in therapeutic gene editing.[5–7] Early intervention into DMD by CRISPR-mediated genome editing before the replacement of muscle cells with fibrotic or adipose tissue allows functional recovery and rescue of abnormalities associated with disease. With this approach, we and others have corrected nonsense mutations in *mdx* and *mdx*^{4cv} DMD mouse models.[8–11] However, single point mutations represent only ~10% of DMD cases, while exon deletion mutations that disrupt the reading frame between adjacent exons are the predominant mutation type, accounting for ~70% of total cases.[12] To investigate exon deletion mutations of the dystrophin gene, several DMD mouse models carrying frame-shifting exon deletion mutations in "hotspot" regions of the gene have been established by CRISPR-Cas9-mediated mutagenesis, including deletion of exons 8, 9, 43, 44, 45, 50, 51, and 52.[13–17] Using adeno-associated virus (AAV) as a delivery vector, CRISPR-Cas gene editing components were delivered to these mouse models and successfully corrected DMD mutations post-natally, further supporting CRISPR-Cas gene editing as a potential therapy for DMD.[13–15,18–20]

Received 19 March 2022; accepted 20 July 2022;
https://doi.org/10.1016/j.omtn.2022.07.024.

Correspondence: Eric N. Olson, PhD. Department of Molecular Biology, University of Texas Southwestern Medical Center, Dallas, TX 75390, USA.
E-mail: eric.olson@utsouthwestern.edu

This is an open access article under the CC BY-NC-ND license (http://creativecommons.org/licenses/by-nc-nd/4.0/).

While the mouse and human dystrophin proteins are highly conserved with respect to exon composition and amino acid sequence, the mouse and human dystrophin genes vary at the genomic level because of codon degeneracy. These nucleotide differences impede direct translation of CRISPR-Cas9 gene editing between DMD animal models and humans since the Cas9 nuclease is guided by sequence-specific single guide RNAs (sgRNAs), and hence human-specific sgRNAs may not efficiently target the mouse genome and thus cannot be tested in DMD mouse models. In this study, we describe the creation of a unique X-linked humanized DMD mouse model in which mouse exon 51 was replaced with human exon 51. Subsequent deletion of mouse exon 50 placed human exon 51 out of frame, generating the *mDmd* ΔEx50; *hDMD* Ex51 knockin humanized DMD mouse model (hereafter referred to as Δ50;h51KI mice).

We then explored the potential of CRISPR-mediated single-cut gene editing using *Staphylococcus pyogenes* Cas9 (*Sp*Cas9) as a means of correcting the human exon 51 out-of-frame mutation in this X-linked humanized DMD model. Systemic delivery of AAV9 vectors expressing an engineered *Sp*Cas9 nuclease and sgRNAs in Δ50;h51KI mice resulted in efficient restoration of dystrophin expression in skeletal muscle and heart and improved muscle contractility. Additionally, we translated this gene editing strategy to restore dystrophin protein expression in DMD patient-derived human cardiomyocytes generated from induced pluripotent stem cells (iPSCs). The establishment of this X-linked humanized DMD mouse model allows rapid sgRNA screening and optimization in human cells and direct translation to animals and, ultimately, patients with DMD.

RESULTS

Generation of humanized DMD mouse model with human exon 51

Previously, using CRISPR-*Sp*Cas9-mediated single-cut gene editing technology, we restored the open reading frame (ORF) of *Dmd* exon 51 in mice and dogs with exon 50 deletion.[13,21] However, due to genomic sequence variations between different species, *in vivo* evaluation of human sgRNAs and editing of the human genome is not possible with the mouse genomic sequence (Figure S1). To address this issue, we first introduced the human exon 51 genomic sequence in mice by CRISPR-*Sp*Cas9-mediated homology-directed repair (HDR) (Figure 1A). These mice, referred to as human exon 51 KI (h51KI) mice, have endogenous mouse exon 51 replaced by 233 bp of human exon 51 on the X chromosome, while mouse introns 50 and 51 remain unchanged. Sequencing of reverse transcription polymerase chain reaction (RT-PCR) amplicons from h51KI mouse triceps muscle confirmed precise splicing of mouse exon 50 with human exon 51 (Figures S2A and S2B). Similar to wild-type (WT) mice, h51KI mice showed membrane localization of the dystrophin protein (Figure S2C), and western blot analysis showed no difference in dystrophin protein expression levels between WT and h51KI mice (Figures S2D and S2E).

Next, we injected zygotes of h51KI mice with two sgRNAs that target the introns flanking mouse exon 50. By genomic sequencing, we identified a F_0 founder mouse with a 216 bp deletion that placed the human exon 51 out of frame and used this mouse line for further studies. We confirmed deletion of mouse exon 50 in the Δ50;h51KI mouse line by RT-PCR using primers targeting mouse exons 49–52 (Figure 1B). Sanger sequencing of the RT-PCR product showed precise splicing of mouse exon 49 with human exon 51, which generates a premature termination codon in human exon 51 (Figure 1C). Histological analysis at 4 weeks of age showed inflammatory infiltration and regenerative muscle fibers with central nuclei in Δ50;h51KI mice (Figure 1D). Absence of dystrophin in muscle membranes was shown in the triceps and heart of Δ50;h51KI mice by immunohistochemistry (Figure 1E). Western blot analysis confirmed complete loss of dystrophin protein expression (Figure 1F). Muscle contraction in the absence of dystrophin tears muscle membranes and releases creatine kinase (CK) into the bloodstream. The serum CK level in Δ50;h51KI mice was elevated 34-fold compared with h51KI mice, indicating muscle damage (Figure 1G). The dystrophic phenotype manifested in Δ50;h51KI mice indicates that this KI humanized DMD mouse line recapitulates DMD pathology seen in other mouse models and can be used as an animal model to develop therapies for DMD.

Strategies for CRISPR-Cas9-mediated gene editing of humanized DMD mice

The Δ50;h51KI mice carry one of the most common genomic deletions seen in patients with DMD. CRISPR-Cas-mediated gene editing of *DMD* exon 51, in principle, could provide therapeutic benefit to ~13% of the population with DMD.[22] We investigated the feasibility of using CRISPR-*Sp*Cas9-mediated single-cut gene editing to correct the human exon 51 out-of-frame mutation. In this strategy, a single sgRNA was used to induce a DNA double-strand break (DSB) between the 5′-AG-3′ splice acceptor and the 5′-TGA-3′ premature termination codon. Non-homologous end-joining (NHEJ) generated genomic insertions and deletions (indels) to repair the DSB. Restoration of dystrophin protein by reframing of exon 51 can be accomplished by indels that insert one nucleotide (3n+1) or delete two nucleotides (3n−2) (Figure 2A). Alternatively, skipping of exon 51 will occur if an indel is large enough to disrupt the 5′-AG-3′ splice acceptor (Figure 2A).

We screened *Sp*Cas9 with sgRNAs in human 293T cells because the Δ50; h51KI mice carry human exon 51. We tested a control sgRNA that was used in previous studies to correct an exon 51 out-of-frame mutation in mice (Figures 2B and S1). This control sgRNA did not induce efficient DNA cutting in human exon 51, as indicated by the low percentage, less than 15%, of total NHEJ events (Figure 2B). Next, we tested two additional sgRNAs (sgRNA-1 and -2) that demonstrated 26%–33% total DNA-cutting activity. However, the productive editing activity, as defined by restoration of the human exon 51 ORF, remained low at 10% (Figure 2B).

To identify an optimal sgRNA with high productive editing, we examined additional *Sp*Cas9 variants with different protospacer adjacent motif (PAM) sequence requirements for DNA cutting.

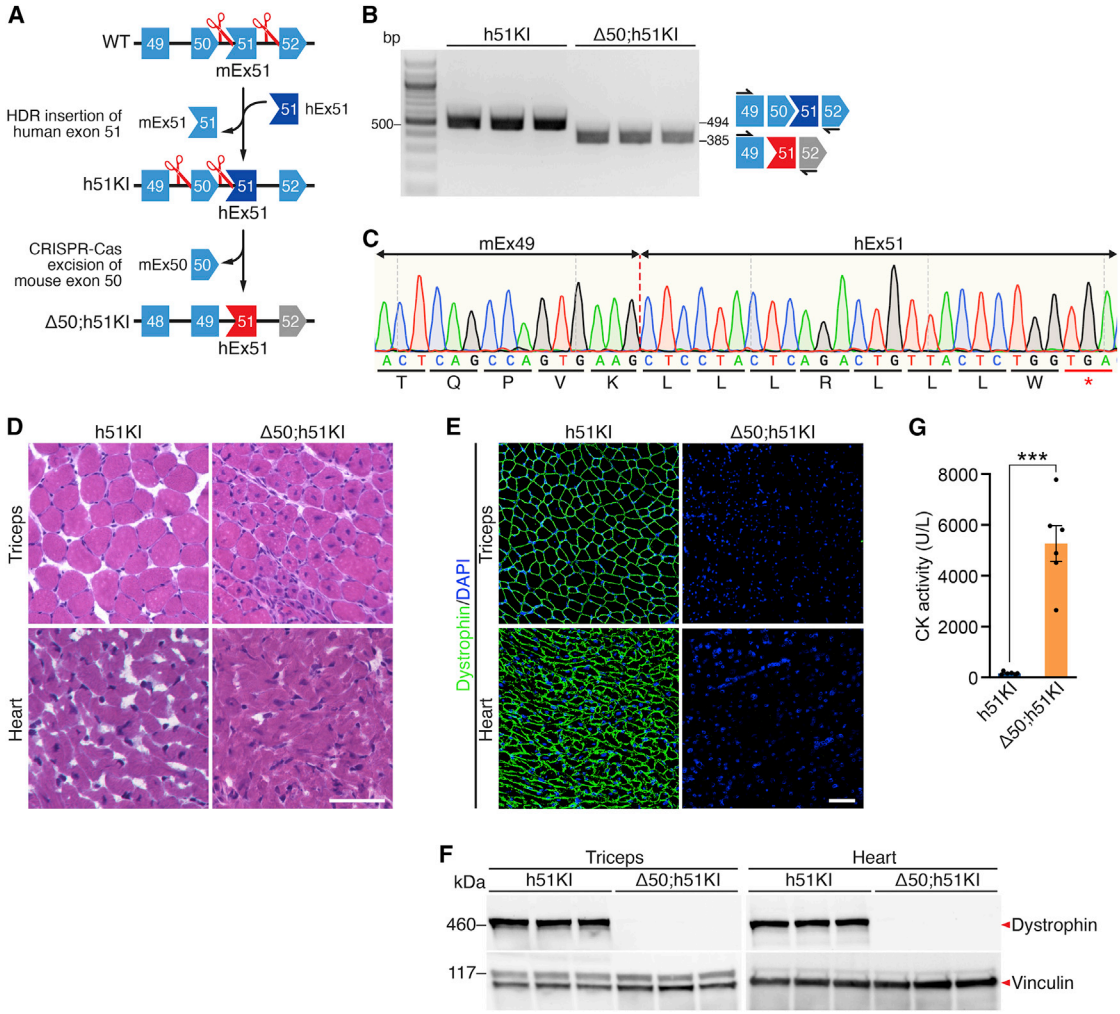

Figure 1. Generation of humanized dystrophic mice with DMD human exon 51 knockin

(A) CRISPR-Cas9-mediated gene targeting to generate humanized dystrophic mice. Mouse exon 51 (mEx51) was replaced by human exon 51 (hEx51) through HDR, generating h51KI mice. Subsequent deletion of mEx50 placed hEx51 out of frame, generating Δ50;h51KI mice. (B) RT-PCR analysis of triceps muscle to validate deletion of mEx50. Primers target mouse exons 49 and 52. Amplicon size is 494 bp for h51KI mice and 385 bp for Δ50;h51KI mice (n = 3). (C) Sanger sequencing of RT-PCR product from the triceps muscle of Δ50;h51KI mice confirms splicing of mEx49 to hEx51. Deletion of mEx50 generates a premature termination codon in hEx51, indicated by a red asterisk. (D) H&E staining of triceps and heart of h51KI and Δ50;h51KI mice. Note centralized nuclei in Δ50;h51KI triceps, indicative of myofiber degeneration and regeneration. Scale bar, 100 μm. (E) Immunohistochemistry of triceps and heart of h51KI and Δ50;h51KI mice. Dystrophin is shown in green. Nuclei are stained with DAPI in blue. Scale bar, 200 μm. (F) Western blot shows complete loss of dystrophin protein expression in triceps and heart of Δ50;h51KI mice. Vinculin is the loading control (n = 3). (G) Serum creatine kinase (CK), an indicator of muscle damage, is abnormally elevated in Δ50;h51KI mice. Data are represented as mean ± SEM. Unpaired two-tailed Student's t tests were performed. ***$p < 0.001$ (n = 6).

*Sp*Cas9-NG and *Sp*Cas9-VRQR nucleases are engineered Cas9 variants carrying amino acid substitutions in the PAM-interacting domain that enable robust genome editing at target sites with a 5′-NGN-3′ PAM or a 5′-NGA-3′ PAM, respectively.[23,24] We screened 7 additional sgRNAs (sgRNA-3 to -9) and discovered that sgRNA-9 coupled with *Sp*Cas9-VRQR nuclease generated the highest productive editing activity (Figure 2B). This optimized sgRNA-9 recognizes a 5′-TGA-3′ PAM in human exon 51 and cuts genomic DNA 11 bp upstream of the premature termination codon (Figure 2C).

Systemic CRISPR-*Sp*Cas9-VRQR gene editing restores dystrophin expression in humanized DMD mice

To assess the efficacy of the *Sp*Cas9-VRQR nuclease and sgRNA-9 *in vivo*, we designed a dual AAV delivery system to package the CRISPR-Cas9 gene editing components individually. AAV serotype 9 (AAV9) was chosen because of its tropism to striated muscle. In this dual AAV delivery system, the *Sp*Cas9-VRQR nuclease was cloned into a single-stranded AAV vector, and its expression was driven by the muscle-specific CK8e promoter (Figure 3A).[25] We chose a double-stranded self-complementary AAV (scAAV) vector

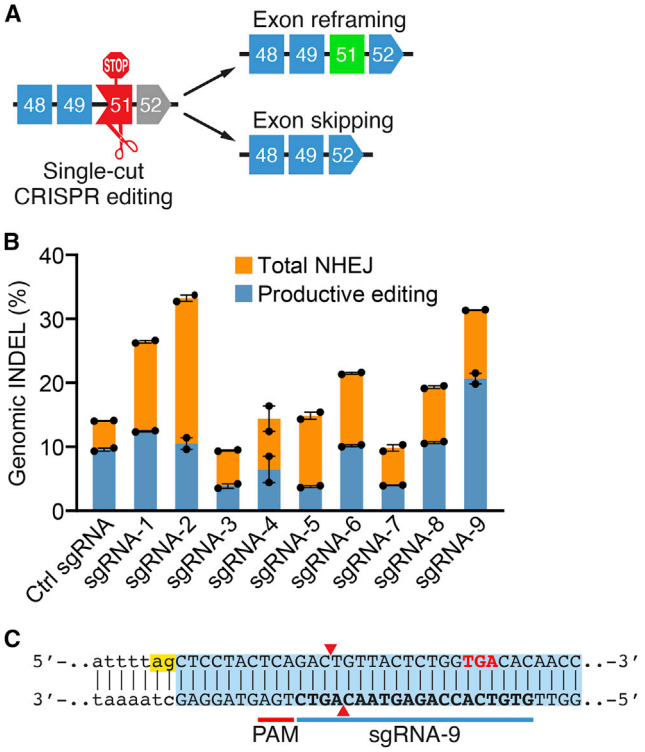

Figure 2. Strategies for CRISPR-Cas9-mediated gene editing of humanized DMD mice

(A) Δ50;h51KI mice have deletion of mEx50, resulting in splicing of mEx49 to hEx51, generating a premature termination codon in hEx51. A CRISPR-Cas9-mediated single-cut gene editing strategy was designed to restore the open reading frame of the dystrophin gene. Small insertions and deletions (indels) with one nucleotide insertion (3n+1) or two nucleotide deletions (3n−2) can reframe hEx51. Large indels disrupting the 5′-AG-3′ splice acceptor sequence cause hEx51 skipping, resulting in splicing of exon 49 to exon 52. (B) *In vitro* screening of CRISPR sgRNAs targeting hEx51. Total NHEJ is defined as total genomic indels after gene editing. Productive editing is defined as indels with 3n+1 insertion or 3n−2 deletion, which are capable of reframing or skipping hEx51. Data are represented as mean ± SEM (n = 2). (C) Illustration of the sgRNA-9 targeting hEx51. This sgRNA recognizes a 5′-TGA-3′ PAM in exon 51 and generates a DSB 11 bp upstream of the premature termination sequence (indicated in red). The 5′-AG-3′ splice acceptor sequence is indicated in yellow. Exon is highlighted in blue. Exon sequence is shown as uppercase letters. Intron sequence is shown as lowercase letters.

to express sgRNA-9 because scAAV showed substantially higher viral transduction efficiency in systemic CRISPR gene editing.[14,19] Moreover, we cloned two copies of the sgRNA-9 expression cassette driven by two RNA polymerase III promoters, U6 and M11, because sgRNA has been shown to be rate limiting for *in vivo* gene editing of DMD mouse models (Figure 3A).[15,26]

To achieve whole-body gene editing, we systemically delivered AAV-*Sp*Cas9-VRQR and AAV-sgRNA-9 to post-natal day 4 (P4) Δ50;h51KI mice through intraperitoneal (i.p.) injection at a dose of 8×10^{13} vector genomes (vg)/kg for each AAV vector. Four weeks after systemic AAV delivery, we assessed dystrophin protein expression in several muscle tissues, including tibialis anterior (TA) of the hindlimb, triceps of the forelimb, diaphragm, and cardiac muscle. Assessment by immunohistochemistry showed extensive dystrophin expression in skeletal muscles and the heart (Figures 3B and S3). Δ50;h51KI mice receiving systemic gene editing displayed 89%, 86%, and 93% dystrophin-positive myofibers in TA, triceps, and diaphragm, respectively (Figure S4). To further quantitatively assess dystrophin protein restoration, we performed western blot analysis in skeletal muscles and the heart of *Sp*Cas9-VRQR gene-edited Δ50;h51KI mice. Mice receiving the systemic AAV treatment restored 18%–26% of WT levels of dystrophin protein in multiple skeletal muscles and heart (Figures 4A and 4B).

To determine the genomic alterations associated with restoration of the dystrophin ORF, we performed deep sequencing analysis on muscles of *Sp*Cas9-VRQR gene-edited Δ50;h51KI mice. Mice receiving systemic administration of AAV-*Sp*Cas9-VRQR and AAV-sgRNA-9 had an average 11%–15% of total indels in skeletal muscles, while genomic indels in the heart reached 17% (Figure 4C). Notably, productive editing events that restored the human exon 51 ORF were the predominant indels in *Sp*Cas9-VRQR gene-edited Δ50;h51KI mice (Figures 4C, S5A, and S5B). Genomic indel analysis of whole muscle tissue may underestimate the CRISPR-Cas9 gene editing efficiency because the other cell types in muscle, such as endothelial cells, inflammatory monocytes, and fibroblasts, are not edited by the muscle-specific *Sp*Cas9-VRQR nuclease. Therefore, by RT-PCR and sequencing, we analyzed dystrophin transcripts at the cDNA level and found reframing events, which included one nucleotide insertion (+T) and two-nucleotide deletion (−GT) as the predominant indels, accounting for 55%–65% of sequence alterations at the cDNA level (Figures 4D and S5C). In addition to reframing events, we observed skipping of human exon 51 at the cDNA level, with an average of 4.5%–12.8% in skeletal muscle and 26.5% in the heart (Figures 4D and S5C). These findings indicate that *Sp*Cas9-VRQR-mediated single-cut gene editing coupled with the optimized CRISPR sgRNA-9 can effectively correct human exon 50 DMD deletion mutations *in vivo*.

Systemic CRISPR-*Sp*Cas9-VRQR gene editing improves muscle function and restores muscle integrity in humanized DMD mice

To examine the effect of dystrophin restoration on muscle integrity and function, we measured serum CK levels, forelimb grip strength, and muscle contractility in *Sp*Cas9-VRQR gene-edited Δ50;h51KI mice. Elevated serum CK is a pathological indicator of muscle damage. Compared with h51KI control mice, the serum CK activity of Δ50;h51KI mice injected with saline was elevated by 33.4-fold. In contrast, the serum CK of *Sp*Cas9-VRQR gene-edited Δ50;h51KI mice was only elevated by 3.2-fold, indicative of muscle protection from contraction-induced damage (Figure 5A). Additionally, we determined whether *Sp*Cas9-VRQR gene editing was able to improve muscle strength in Δ50;h51KI mice. The grip strength of Δ50;h51KI mice receiving saline was reduced by 45% compared with h51KI control mice (Figure 5B). In contrast, the grip strength of Δ50;h51KI mice

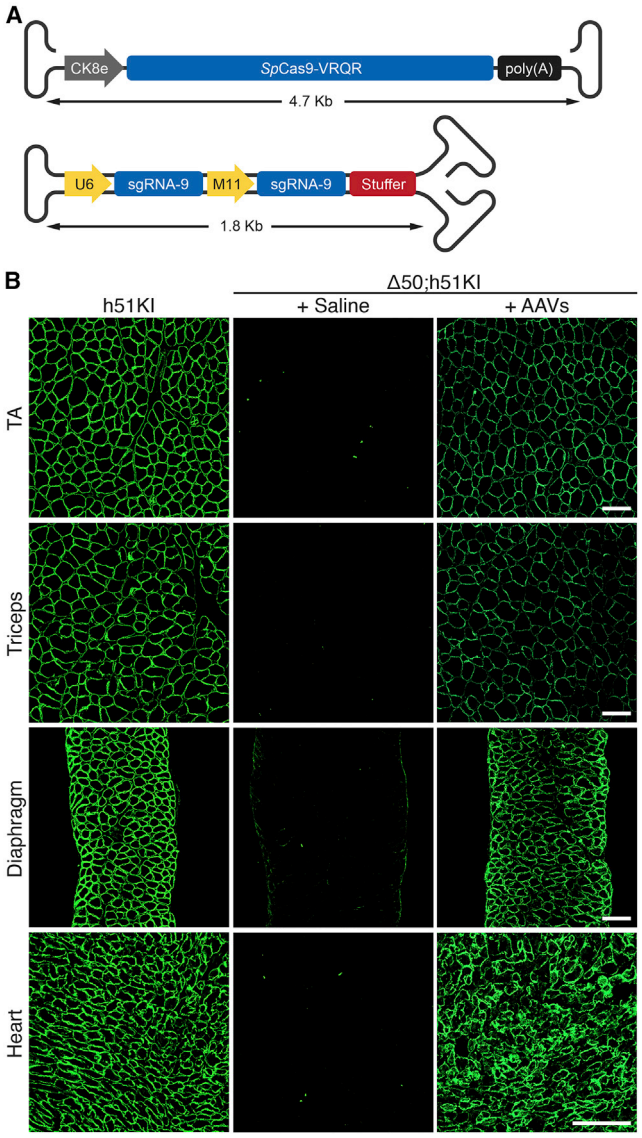

Figure 3. Systemic delivery of *Sp*Cas9-VRQR gene editing components restores dystrophin expression in humanized DMD mice

(A) Illustration of AAV vectors used to deliver *Sp*Cas9-VRQR nuclease and sgRNAs. *Sp*Cas9-VRQR nuclease was cloned into a single-stranded AAV backbone, and its expression was driven by the muscle-specific CK8e promoter. Two copies of the sgRNA-9 targeting hEx51 were cloned into a double-stranded self-complementary AAV backbone. sgRNA expression was driven by two RNA polymerase III promoters, U6 and M11. A stuffer sequence was cloned into the sgRNA-expression AAV vector for optimal viral packaging. (B) Immunohistochemistry shows restoration of dystrophin in the tibialis anterior (TA), triceps, diaphragm, and heart of Δ50;h51KI mice after systemic delivery of AAV-*Sp*Cas9-VRQR (8×10^{13} vg/kg) and AAV-sgRNA-9 (8×10^{13} vg/kg). Delivery age, P4; analysis age, 4 weeks. Dystrophin is shown in green. Scale bars, 100 μm (n = 6 for each muscle group, one representative image is presented for each muscle group).

receiving systemic AAV-*Sp*Cas9-VRQR and AAV-sgRNA-9 was only reduced by 11% compared with h51KI control mice (Figure 5B).

To evaluate whether systemic CRISPR-*Sp*Cas9-VRQR gene editing was able to rescue the pathological phenotype seen in Δ50;h51KI mice, we performed hematoxylin and eosin (H&E) staining of skeletal muscles and the heart isolated from Δ50;h51KI mice. In the saline-treated control group, Δ50;h51KI mice displayed centralized nuclei, necrosis, and inflammatory infiltration in TA, triceps, and diaphragm muscles (Figures S6 and S7). The percentage of regenerating myofibers with central nuclei in saline-treated Δ50;h51KI mice was between 26% and 45% across different skeletal muscle groups (Figure S8). After systemic CRISPR-*Sp*Cas9-VRQR gene editing, the percentage of centralized nuclei in myofibers declined substantially (Figure S8). Together, these findings demonstrate that *Sp*Cas9-VRQR-mediated single-cut gene editing improves muscle integrity and provides functional benefit to Δ50;h51KI mice.

Next, we performed muscle contraction analysis on soleus and extensor digitorum longus (EDL) muscles isolated from Δ50;h51KI mice 4 weeks after receiving systemic AAV-*Sp*Cas9-VRQR and AAV-sgRNA-9. In the cohort administered saline, the force of soleus and EDL was reduced by 58% and 43%, respectively, compared with h51KI control mice (Figures 5C and 5D). After systemic CRISPR-*Sp*Cas9-VRQR gene editing, the force exhibited by soleus and EDL was increased by 82% and 47%, respectively, compared with the saline control group (Figures 5C and 5D). A similar pattern was seen for maximal tetanic force of treated soleus and EDL (Figures 5E and 5F). Improvement of muscle contraction in soleus and EDL correlated with increased dystrophin expression and decreased muscle degeneration (Figures S9 and S10).

*Sp*Cas9-VRQR gene editing restores dystrophin expression and shows minimal off-target editing in patient iPSC-derived ΔEx48-50 cardiomyocytes

To investigate whether efficient gene editing in humanized mice is translatable to human DMD cardiomyocytes, we performed *Sp*Cas9-VRQR-mediated single-cut gene editing in human iPSCs generated from a patient with ΔEx48-50 DMD (Figure 6A). This DMD iPSC line carries an out-of-frame deletion of multiple *DMD* exons, spanning from exon 48 to 50, which generates a premature termination codon in exon 51. We used the same sgRNA-9 that showed high efficiency in humanized DMD mice to correct the mutation in ΔEx48-50 iPSCs. From immunocytochemistry and western blot analysis, we found that cardiomyocytes differentiated from *Sp*Cas9-VRQR gene-edited ΔEx48-50 iPSC mixtures (ΔEx48-50 iPSC-cardiomyocytes [CMs]) showed a high level of dystrophin protein expression comparable to healthy control CMs, even without clonal selection and expansion (Figures 6B and 6C). To assess the potential off-target effects of *Sp*Cas9-VRQR-mediated gene editing, we performed deep sequencing analysis on the top four off-target sites. We did not observe significant genomic modifications across any of the off-target sites (Figure 6D; Table S2). We conclude that *Sp*Cas9-VRQR-mediated single-cut gene editing represents an

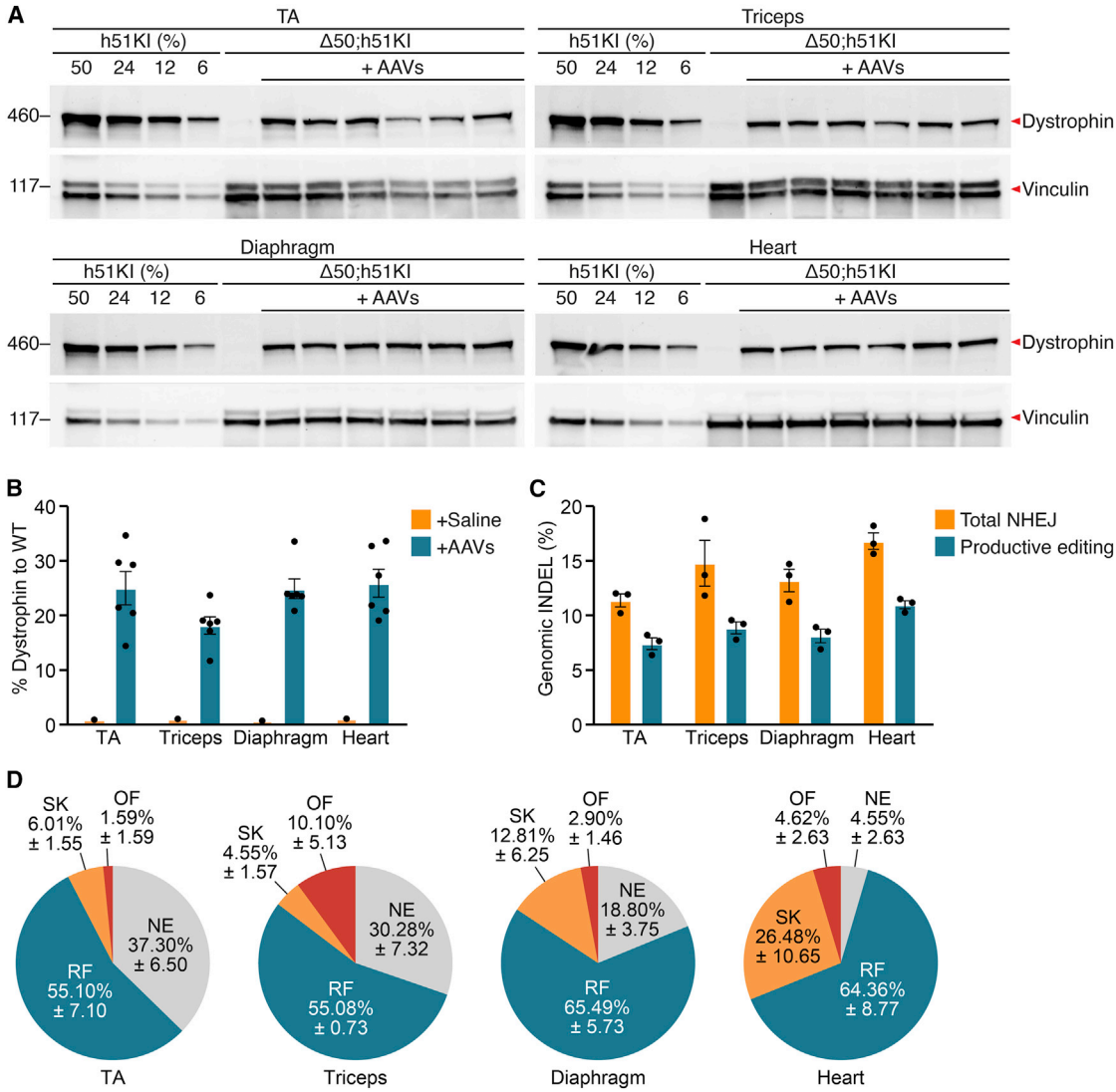

Figure 4. Restoration of dystrophin protein expression in humanized DMD mice after systemic delivery of *Sp*Cas9-VRQR gene editing components

(A) Western blot analysis shows restoration of dystrophin protein expression in the TA, triceps, diaphragm, and heart of AAV-*Sp*Cas9-VRQR and AAV-sgRNA-9 gene-edited Δ50;h51KI mice. Dilutions of protein extract from muscle tissues of h51KI control mice, expressed as percentage of protein input, serve to standardize dystrophin protein expression. Vinculin was used as the loading control (n = 6). (B) Quantification of dystrophin protein expression in the TA, triceps, diaphragm, and heart of saline-treated and AAV-*Sp*Cas9-VRQR and AAV-sgRNA-9 gene-edited Δ50;h51KI mice. Relative dystrophin intensity was calibrated with vinculin internal control before normalizing to the h51KI control mice. Data are represented as mean ± SEM (n = 6). (C) Deep sequencing analysis of genomic indels in the TA, triceps, diaphragm, and heart of Δ50;h51KI mice after systemic delivery of AAV-*Sp*Cas9-VRQR and sgRNA-9. Data are represented as mean ± SEM (n = 3). (D) Analysis of cDNA indels in the TA, triceps, diaphragm, and heart of Δ50;h51KI mice after systemic delivery of AAV-*Sp*Cas9-VRQR and AAV-sgRNA-9. NE, not edited; RF, exon 51 reframed; SK, exon 51 skipped; OF, out of frame. Data are represented as mean ± SEM (n = 3). All measurements were performed 4 weeks after systemic delivery of AAV-*Sp*Cas9-VRQR (8×10^{13} vg/kg) and AAV-sgRNA-9 (8×10^{13} vg/kg); delivery age, P4.

efficient and safe strategy to correct human exon 51 out-of-frame mutations in both humanized DMD mice and human DMD iPSCs.

DISCUSSION

Despite extensive efforts to develop CRISPR-Cas-mediated therapeutic gene editing to correct DMD mutations, challenges remain in testing human-specific CRISPR sgRNAs in animal models because of genomic sequence variations between species. By truncating two nucleotides in the PAM-distal region of a sgRNA, we were able to find a conserved 18-nucleotide sgRNA that efficiently corrects DMD exon 45 mutations in human CMs and mice.[15,19] However, this approach cannot be universally applied to other dystrophin exons, such as exon 51, because sgRNAs targeting human or mouse exon 51 have sequence variations in the PAM-proximal region or at the PAM site.

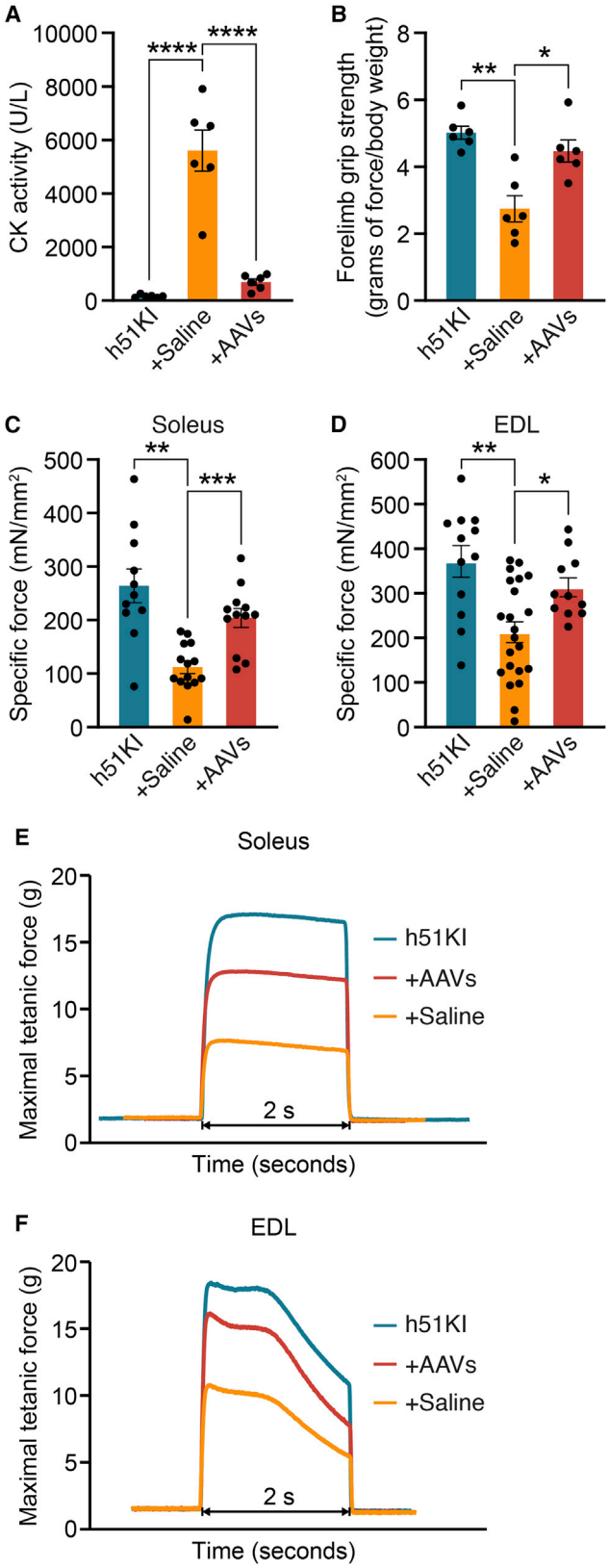

Figure 5. Systemic *Sp*Cas9-VRQR-mediated single-cut gene editing improves muscle function in humanized DMD mice

(A) Serum CK measurements in h51KI control mice, saline-treated, and AAV-*Sp*Cas9-VRQR, AAV-sgRNA-9 gene-edited Δ50;h51KI mice. Data are represented as mean ± SEM. One-way ANOVA was performed with post-hoc Tukey's multiple comparisons test. ****$p < 0.0001$ (n = 6). (B) Forelimb grip-strength analysis of h51KI control mice, saline-treated, and AAV-*Sp*Cas9-VRQR, AAV-sgRNA-9 gene-edited Δ50;h51KI mice. Grams of force is normalized with body weight. Data are represented as mean ± SEM. One-way ANOVA was performed with post-hoc Tukey's multiple comparisons test. *$p < 0.05$, **$p < 0.01$ (n = 6). (C and D) Specific force (mN/mm^2) of the soleus (C) and extensor digitorum longus (EDL) (D) muscles of h51KI control mice, saline treated, and AAV-*Sp*Cas9-VRQR, AAV-sgRNA-9 gene edited Δ50;h51KI mice. Data are represented as mean ± SEM. One-way ANOVA was performed with post-hoc Tukey's multiple comparisons test. *$p < 0.05$, **$p < 0.005$, ***$p < 0.001$ (n = 10 for analysis of EDL muscle of saline-treated Δ50;h51KI mice, n = 6 for other treatments). (E and F) Maximal tetanic force of the soleus (E) and EDL (F) muscles of h51KI control mice, saline-treated, and AAV-*Sp*Cas9-VRQR, AAV-sgRNA-9 gene-edited Δ50;h51KI mice (n = 10 for analysis of EDL muscle of saline treated Δ50;h51KI mice, n = 6 for other treatments, one representative trace image is presented for each group). All measurements were performed 4 weeks after systemic delivery of AAV-*Sp*Cas9-VRQR (8×10^{13} vg/kg) and AAV-sgRNA-9 (8×10^{13} vg/kg); delivery age, P4.

Previously, two humanized DMD mouse models were established by integrating the full-length human *DMD* gene into mouse chromosome 5 and deleting human *DMD* exon 45 or 52 in embryonic stem cells isolated from the mouse model.[27,28] When backcrossed to *mdx* mice, these transgenic humanized DMD mice displayed muscular dystrophy. However, a recent study revealed that these humanized DMD mice carry two copies of the human *DMD* transgene at the integration locus in a tail-to-tail orientation, making this DMD mouse model unsuitable for testing *in vivo* CRISPR-Cas9 gene editing.[29] This is because the sgRNA can cut twice in the human *DMD* transgenes, which may generate unwanted chromosomal alterations, including large deletions, inversions, or translocations. In contrast, the humanized DMD mouse model created in this study contains mouse exon 51 replaced by its human ortholog within the endogenous genomic location on the X chromosome. Subsequent deletion of mouse exon 50 puts the human exon 51 out of frame and generates a dystrophic DMD mouse model that represents the most common genomic deletions seen in patients with DMD. In addition, this X-linked humanized DMD mouse model transcribes the chimeric dystrophin gene from the endogenous promoter and faithfully segregates the mouse *Dmd* gene with human *DMD* exon 51 in an X-chromosome-dependent manner without the need to cross with other dystrophic mice.

The WT *Sp*Cas9 nuclease prefers a 5′-NGG-3′ PAM for efficient gene editing.[30] The sgRNAs used for correcting *Dmd* exon 51 out-of-frame mutations in mice and dogs utilize the 5′-TGG-3′ PAM for DNA cutting, which is a canonical PAM for the WT *Sp*Cas9. However, the PAM sequence for the corresponding sgRNA targeting human exon 51 is 5′-TAG-3'. This 5′-NAG-3′ PAM is not an optimal PAM for WT *Sp*Cas9, rendering gene editing of human exon 51 less efficient. In this study, we devised an efficient single-cut gene editing method using an engineered *Sp*Cas9-VRQR nuclease to restore the human

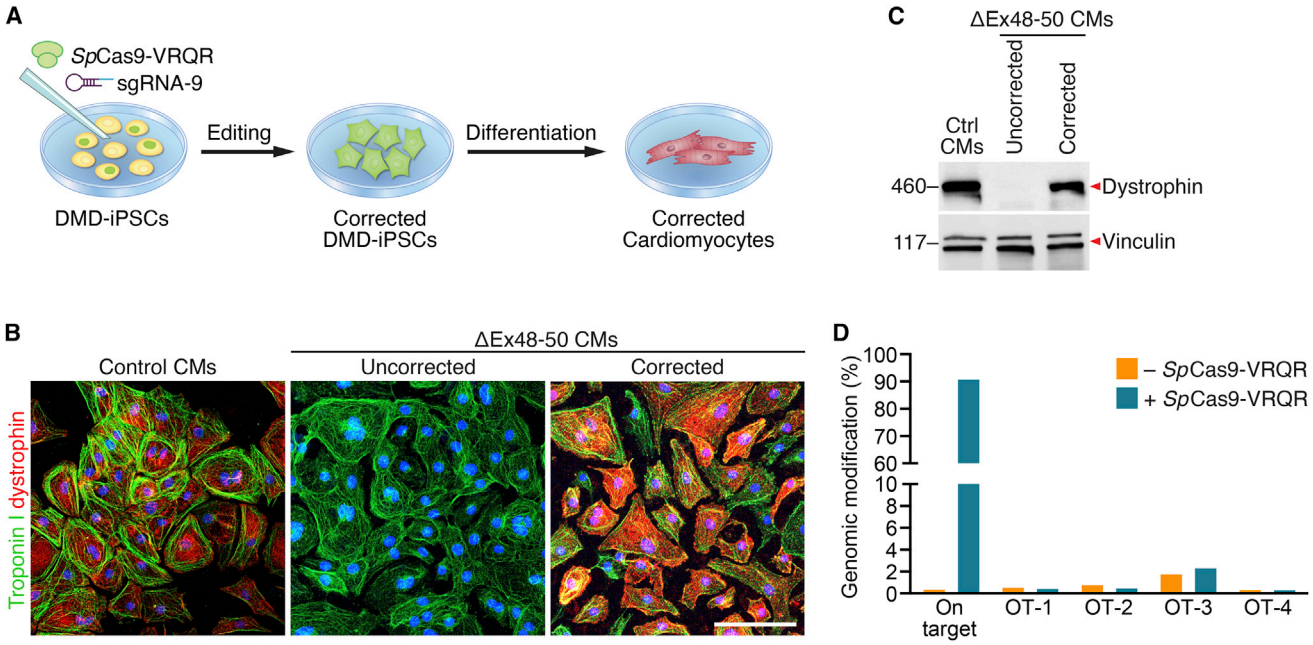

Figure 6. *Sp*Cas9-VRQR-mediated single-cut gene editing restores dystrophin expression in patient iPSC-derived DMD ΔEx48-50 cardiomyocytes

(A) DMD ΔEx48-50 iPSCs were edited by *Sp*Cas9-VRQR gene editing components (corrected DMD iPSCs) and then differentiated into corrected cardiomyocytes (CMs) for downstream analysis. (B) Immunocytochemistry shows dystrophin restoration in mixtures of DMD ΔEx48-50 CMs following *Sp*Cas9-VRQR-mediated single-cut gene editing. Red, dystrophin immunostaining; green, troponin I immunostaining. Scale bar, 100 μm. (C) Western blot shows dystrophin protein restoration in mixtures of DMD ΔEx48-50 CMs following *Sp*Cas9-VRQR-mediated single-cut gene editing. Vinculin was used as the loading control. (D) Genomic deep sequencing analysis of the on-target and top four predicted off-target sites of *Sp*Cas9-VRQR sgRNA-9. OT, off-target.

exon 51 ORF. *Sp*Cas9-VRQR utilizes a 5′-NGA-3′ PAM for DNA cutting.[23] By screening several sgRNAs, we identified an optimal sgRNA with a 5′-TGA-3′ PAM in human cells and translated *Sp*Cas9-VRQR-mediated single-cut gene editing in Δ50;h51KI mice and observed a high percentage of productive editing in this humanized DMD mouse model while manifesting minimal off-target editing based on amplicon sequencing. To further ensure clinical safety in the future, it would be beneficial to perform unbiased off-target analyses, such as SITE-seq or GUIDE-seq, to systematically interrogate potential off-target activities.[31,32] Therefore, the Δ50;h51KI humanized DMD mice established in this study bring compatibility between *in vitro* screening of sgRNAs in human cells and *in vivo* assessment of gene-editing efficacy in animals.

In this study, Δ50;h51KI humanized DMD mice were established by deleting mouse exon 50 in h51KI WT mice. This KI humanized mouse model can be used to test different CRISPR-Cas-based gene editing strategies that target human exon 51. This mouse model can also be used to test other therapeutic approaches for DMD, such as antisense oligonucleotide-based exon skipping and microdystrophin-based gene replacement. Using h51KI WT mice as a starting point, additional humanized DMD mice can be generated, such as mice with exon 52 deletion mutation (Δ52;h51KI mice) and mice with exon 46–50 deletion mutation (Δ46-50;h51KI mice). Different editing strategies can be deployed to correct these mutations. Specifically, a mutation in Δ52;h51KI mice can be corrected by one nucleotide insertion (3n+1) or two nucleotide deletions (3n−2) at the 3′ end of human exon 51, while a mutation in Δ46-50;h51KI mice can be corrected by two nucleotide insertions (3n+2) or one nucleotide deletion (3n−1) at the 5′ end of human exon 51. However, the humanized DMD mouse model developed in this study only contains human exon 51, while other exons remain mouse sequences, which limits its application in CRISPR-Cas-based gene editing of other exons. In the future, it would be useful to establish additional humanized DMD mouse models by knocking in other human exons.

CRISPR-Cas-mediated gene editing has shown promise in treating DMD in preclinical studies, although several questions and challenges remain to be addressed. One concern is the immune response elicited by the Cas9 nuclease. Preclinical studies in DMD dog models using AAV-delivered *Sa*Cas9 or *Sp*Cas9 showed different gene editing outcomes. A short-term study in AAV9-*Sp*Cas9-mediated gene editing of DMD dogs with exon 50 deletion showed highly efficient dystrophin protein restoration without significant CD4- or CD8-positive cell infiltration in skeletal muscles.[21] In contrast, another study of AAV8-*Sa*Cas9- or -*Sp*Cas9-mediated gene editing of DMD dogs with mutations in introns 6, 13, and 19 reported Cas9-specific humoral and cytotoxic T lymphocyte responses, leading to loss of dystrophin-positive myofibers.[33] *Sp*Cas9 and *Sa*Cas9 nucleases are derived from *Streptococcus pyogenes* and *Staphylococcus aureus*, which infect

the human population at high frequencies.[34] Therefore, there might be a high prevalence of preexisting adaptive immunity to these Cas9 nucleases. Potential solutions to reduce Cas9-specific immune responses include (1) screening Cas orthologs from other bacterial systems with less human exposure; (2) designing a tunable CRISPR-Cas system to turn off Cas nuclease expression after completion of gene editing; (3) extending immunosuppressant supplementation to alleviate immune responses; and (4) establishing immune tolerance to Cas9 by generating Cas9-specific regulatory T cells.[35,36] The single-cut gene editing strategy deployed in this study is able to restore 20%–25% of dystrophin protein in skeletal muscle and heart. However, this strategy relies on NHEJ-mediated reframing, which generates small genomic indels around the cut site. Dystrophin protein restored by exon reframing may have alternations of amino acid residues around the reframed exon. This alteration may create a neoantigen, which presents potential safety challenges in clinical application of the single-cut reframing strategy for DMD treatment. In the future, it would be instructive to use the humanized DMD mouse model to interrogate potential immune responses triggered by a dystrophin-specific neoantigen.

Another limitation of this study is the high dose of AAV used, which may restrict its clinical application and commercialization. It has been reported that systemic administration of high-dose AAV in large animals may cause acute liver damage.[37,38] Two recent studies showed that screening or engineering a novel AAV capsid with higher muscle tropism and lower liver tropism may reduce the AAV dose used in systemic delivery and potentially prevent liver toxicity.[39,40] In addition, a novel AAV capsid may also prevent potential AAV immunity. The Cas9 nuclease used in this study is derived from *Sp*Cas9, which contains over 1,300 amino acids. Therefore, two AAV vectors are required to separately package Cas nuclease and sgRNA, which increases production cost and the total AAV dose used in gene therapy. In the future, it would be instructive to test other smaller Cas orthologs, such as *Slug*Cas9 or *Sauri*Cas9, in editing human exon 51.[41,42] This could allow consolidation of the entire CRISPR-Cas gene editing system into a single AAV vector and subsequently lower the AAV dose and production cost.

Complete restoration of dystrophin protein to normal levels is not achievable with gene editing because CRISPR-Cas9-mediated editing of myonuclei is not 100% efficient. Prior studies in patients with Becker muscular dystrophy have estimated that ~15% of normal levels of dystrophin protein could provide therapeutic benefits.[43] In this study, we showed that *Sp*Cas9-VRQR-mediated gene editing in Δ50;h51KI mice restored 20%–25% of dystrophin protein in multiple skeletal muscles and heart within 4 weeks of systemic AAV delivery, indicating a beneficial therapeutic outcome of DMD gene editing. It is likely that higher levels of dystrophin protein expression will be achieved after longer-term editing. Repeated cycles of muscle degeneration and regeneration cause replacement of muscle cells with fibrotic and adipose tissues. Therefore, early intervention of DMD using CRISPR-Cas gene editing may provide better therapeutic benefit. In this study, we performed systemic CRISPR-Cas gene editing in P4 mice before the onset of DMD pathology. In the future, additional studies in older mice manifesting DMD pathology would also be informative in evaluating CRISPR-Cas gene editing as a therapy for treating patients with more advanced DMD.

In summary, the Δ50;h51KI humanized DMD mice described in this study, combined with the optimized *Sp*Cas9-VRQR-mediated single-cut gene editing, should facilitate clinical translation of CRISPR-Cas gene editing as a means of permanent correction of DMD in humans.

MATERIALS AND METHODS

Study design

This study was designed with the primary aim of generating an X-linked humanized DMD mouse model with an exon 50 deletion mutation. The secondary objective was to investigate the feasibility of using *Sp*Cas9-VRQR for therapeutic gene editing of this humanized DMD mouse model. Male mice were used in this study. Blind approaches were used for immunostaining analysis, histology validation, grip-strength test, CK measurement, and muscle electrophysiology. For each experiment, the sample size reflects the number of independent biological replicates and was provided in the figure legends. Each animal group (WT, saline treated, and AAV treated) has at least 6 mice (n = 6). Each group of mice are from 2 to 3 different litters.

Mice

Δ50;h51KI mice were generated in the B6C3F1 background (a cross between female C57BL/6NCrl and male C3H/HeNCrl) by two rounds of CRISPR-Cas9-mediated gene targeting. In the first round of gene targeting, mouse exon 51 was replaced by human exon 51 through HDR, generating h51KI mice. In the second round of gene targeting, mouse exon 50 was excised by two sgRNAs, placing human exon 51 out of frame and generating Δ50;h51KI mice. CRISPR sgRNAs were synthesized and purchased from Integrated DNA Technologies; Cas9 mRNA was purchased from TriLink Biotechnologies. Injection procedures were performed as described previously.[9] The injection solution comprises CRISPR sgRNAs (20 ng/μL), Cas9 mRNA (50 ng/μL), and HDR template (10 ng/μL circular plasmid). CRISPR sgRNAs used in zygote injections are listed in Table S3. Δ50;h51KI mice were backcrossed with C57BL/6NCrl mice for more than four generations. Genotyping primers are listed in Table S3.

*Sp*Cas9-VRQR vector cloning and AAV vector production

The C terminus of *Sp*Cas9-VRQR was synthesized as gBlocks (Integrated DNA Technologies) and subcloned into NheI-HF and BsmI digested p458 VQR plasmid, a gift from A. Holland (Addgene plasmid #101727), using In-Fusion Cloning Kit (Takara Bio), generating the p*Sp*Cas9-VRQR-2A-GFP plasmid. CRISPR sgRNAs targeting human exon 51 were subcloned into the newly designed p*Sp*Cas9-VRQR-2A-GFP plasmid, p*Sp*Cas9-NG-2A-GFP plasmid, or p*Sp*Cas9-WT-2A-GFP plasmid using BbsI digestion and T4 ligation. Sequence information for all sgRNAs is listed in Table S1.

The *Sp*Cas9-VRQR AAV plasmid was generated by subcloning of the C-terminal *Sp*Cas9-VRQR PCR fragment into the KflI and ClaI digested ssAAV-CK8e-WT-*Sp*Cas9 plasmid, generating the ssAAV-CK8e-*Sp*Cas9-VRQR plasmid. Muscle-specific CK8e promoter (a gift from S. Hauschka) was chosen for driving Cas9 expression. The CRISPR sgRNA AAV plasmid was generated by subcloning the U6 and M11 sgRNA expression cassettes into the KpnI-HF and MluI-HF digested pSJG-CBH scAAV plasmid (a gift from S. Gray), generating the scAAV-U6-M11-sgRNA plasmid. A 1.2 kb stuffer sequence was cloned into the scAAV-U6-M11-sgRNA plasmid for optimal AAV packaging. Cloning primer sequences are listed in Table S3. AAV viral plasmids were column purified and digested with SmaI and AhdI to check inverted terminal repeat (ITR) integrity. AAVs were packaged by Boston Children's Hospital Viral Core, and serotype 9 was chosen for capsid assembly. AAV titer was determined by quantitative real-time PCR assay.

In vitro CRISPR sgRNA screening

CRISPR sgRNA screening was performed in human 293T cells by transient transfection. Briefly, 2×10^6 cells were transfected with 3 ug p*Sp*Cas9-VRQR-2A-GFP plasmid, p*Sp*Cas9-NG-2A-GFP plasmid, or p*Sp*Cas9-WT-2A-GFP plasmid cloned with individual sgRNA with 7.5 μL Lipofectamine 2000 transfection reagent according to the manufacturer's protocol. Seventy-two hours post-transient transfection, cells were harvested for genomic DNA extraction. Genomic PCR was performed to amplify the CRISPR-Cas9-edited human *DMD* exon 51 locus. Indel efficiency was analyzed by TIDE analysis.[44]

Human iPSC maintenance, nucleofection, and differentiation

DMD ΔEx48-50 iPSCs (RBRC-HPS0164) were purchased from Cell Bank RIKEN BioResource Center. Stem cell work described in this manuscript was conducted under the oversight of the UT Southwestern Stem Cell Research Oversight (SCRO) Committee. Human iPSCs were cultured in mTeSR plus medium (STEMCELL Technologies) and passaged once reaching 70% confluence (1:18 split ratio). One hour before nucleofection, DMD ΔEx48-50 iPSCs were pretreated with 10 μM ROCK inhibitor (Y-27632) and dissociated into single cells using Accutase (Innovative Cell Technologies). DMD ΔEx48-50 iPSCs (1×10^6) were mixed with 5 μg p*Sp*Cas9-VRQR-2A-GFP-U6-sgRNA-9 plasmid and then nucleofected with the P3 Primary Cell 4D-Nucleofector X Kit (Lonza) according to the manufacturer's protocol. After nucleofection, DMD ΔEx48-50 iPSCs were cultured in mTeSR plus medium supplemented with 10 μM ROCK inhibitor and Primocin (100 μg/mL; InvivoGen). Three days after nucleofection, GFP+ cells were sorted by fluorescence-activated cell sorting (FACS) and subjected to differentiation to CMs and TIDE analysis, as previously described.[14]

In vivo AAV delivery into Δ50;h51KI mice

P4 Δ50;h51KI mice (body weight ~3 g) were injected i.p. with 80 μL saline or AAV9 containing ssAAV2/9-*Sp*Cas9-VRQR (8×10^{13} vg/kg) and scAAV2/9-U6-M11-sgRNAs (8×10^{13} vg/kg) using an ultrafine BD insulin syringe (Becton Dickinson). Four weeks after systemic delivery, Δ50;h51KI mice and h51KI control mice were dissected for physiological, biochemical, and histological analysis. Animal work described in this manuscript was approved and conducted under the oversight of the University of Texas Southwestern Institutional Animal Care and Use Committee.

Genomic DNA and RNA isolation, cDNA synthesis, and PCR amplification

According to the manufacturer's protocol, genomic DNA of human 293T cells and DMD ΔEx48-50 iPSCs was isolated using Quick-DNA Miniprep Plus Kit (Zymo Research); genomic DNA of skeletal muscles and hearts of Δ50;h51KI mice and h51KI control mice was isolated using DNeasy Blood and Tissue Kit (QIAGEN); total RNA of skeletal muscles and heart of Δ50;h51KI mice and h51KI control mice was isolated using miRNeasy Kit (QIAGEN); cDNA was reverse transcribed from total RNA using iScript Reverse Transcription Supermix (Bio-Rad). Genomic DNA and cDNA were PCR amplified using LongAmp Taq DNA Polymerase (New England Biolabs) PCR products were sequenced and analyzed by TIDE analysis.[44] Primer sequences are listed in Table S3.

Dystrophin immunocytochemistry and immunohistochemistry

Immunocytochemistry of iPSC-derived CMs was performed as previously described.[45] In brief, iPSC-derived CMs were fixed with acetone, blocked with serum cocktail (2% normal horse serum, 2% normal donkey serum, 0.2% bovine serum albumin [BSA] in phosphate-buffered saline [PBS]), and incubated with a dystrophin antibody (MANDYS8, 1:800; Sigma-Aldrich) and troponin I antibody (H170, 1:200; Santa Cruz Biotechnology) in 0.2% BSA/PBS. Following overnight incubation at 4°C, CMs were incubated with secondary antibodies (biotinylated horse anti-mouse immunoglobulin G [IgG], 1:200; Vector Laboratories) and fluorescein-conjugated donkey anti-rabbit IgG (1:50; Jackson ImmunoResearch) for 1 h. Nuclei were counterstained with DAPI (1:250; Sigma-Aldrich).

Immunohistochemistry of skeletal muscles and heart of Δ50;h51KI mice and h51KI control mice was performed as previously described.[15] In brief, skeletal muscles and heart of h51KI and Δ50;h51KI mice were cryosectioned into 8 μm transverse sections and delipidated in 1% Triton X-100 in PBS (pH 7.4). Following delipidation, sections were incubated with mouse IgG blocking reagent (M.O.M. Kit, Vector Laboratories), washed, and sequentially equilibrated with M.O.M diluent (600 uL of M.O.M Protein Concentrate stock solution to 7.5 mL of PBS [pH 7.4]). Sections were then incubated with mouse anti-dystrophin primary antibody (MANDYS8, 1:800; Sigma-Aldrich) and rabbit anti-laminin primary antibody (L9393, 1:500; Sigma-Aldrich) dissolved in M.O.M. diluent at room temperature for 1 h. Followed by PBS wash, sections were then incubated with Avidin D conjugated with fluorescein isothiocyanate (FITC; 1:250; Vector Laboratories), goat anti-rabbit IgG secondary antibody conjugated with Alexa Fluor 555 (1:500; Thermo Fisher Scientific), and DAPI (1:250; Sigma-Aldrich) dissolved in M.O.M. diluent at room temperature for 30 min.

Dystrophin western blot analysis

For western blot analysis of iPSC-derived CMs, 4×10^6 cells were lysed in lysis buffer (10% SDS, 62.5 mM tris-HCl [pH 6.8], 1 mM EDTA, and protease inhibitor). Heart and skeletal muscles of Δ50;h51KI mice and h51KI control mice were crushed into fine powder using a liquid-nitrogen-frozen crushing apparatus and lysed in the same lysis buffer as iPSC-derived CMs. Protein concentration was determined by Pierce BCA Protein Assay Kit according to manufacturer's protocol. A total of 40 μg protein was loaded onto 4%–20% Criterion TGX Precast Midi Protein Gel (Bio-Rad). Gels were run at 80 V for 30 min and switched to 130 V for 2 h, followed by a wet transfer to a polyvinylidene difluoride (PVDF) membrane at 100 V at 4°C for 90 min. For dystrophin protein detection, the PVDF membrane was blocked in blocking buffer (5% w/v nonfat dry milk, 1× TBS, 0.1% Tween 20) at room temperature for 1 h and incubated with mouse anti-dystrophin primary antibody (MANDYS8, 1:1,000; Sigma-Aldrich) at 4°C overnight, followed by incubation with goat anti-mouse IgG (H + L)-HRP secondary antibody (1:10,000; Bio-Rad) at room temperature for 1 h. For vinculin protein detection, the PVDF membrane was cleared with stripping buffer and blocked with blocking buffer at room temperature for 1 h. Then, the PVDF membrane was incubated with mouse anti-vinculin primary antibody (V9131, 1:1,000; Sigma-Aldrich) at room temperature for 1 h, followed by incubation with goat anti-mouse IgG (H+L)-HRP secondary antibody (1:10,000; Bio-Rad) at room temperature for 1 h. The PVDF membrane was developed by Western Blotting Luminol Reagent (Santa Cruz) according to manufacturer's protocol and imaged by digital imager (Bio-Rad).

Amplicon deep sequencing analysis

A first round of genomic PCR was performed to amplify on- and off-target sites with adaptor sequence introduced. A second round of PCR was performed to add Illumina flow cell binding sequence and barcodes. All samples were pooled at equal molar ratios and sent for deep sequencing using MiSeq v3 flow cells (22 million reads total). All primer sequences are listed in Table S3. Deep sequencing data was analyzed using CRISPResso2 (https://github.com/pinellolab/crispresso2).

Grip-strength test and serum CK measurement

Forelimb-muscle strength of 4-week-old Δ50;h51KI mice and h51KI control mice was assessed by the grip-strength meter (Columbus Instruments). In brief, an individual mouse was weighed and lifted by the tail, causing the forelimbs to grasp the pull-bar assembly connected to the grip-strength meter. The mouse was drawn along a straight line leading away from the sensor until the grip was broken, and the peak amount of force in grams was recorded. Measurement of forelimb grip strength of each mouse was repeated 5 times in a blinded experimental design. Serum CK was measured by the Metabolic Phenotyping Core at UT Southwestern Medical Center using the VITROS 250 Chemistry System in a blinded experimental design.

Electrophysiological analysis of isolated soleus and EDL muscles

Four weeks after systemic AAV9-*Sp*Cas9-VRQR gene editing, soleus and EDL muscles of h51KI mice and Δ50;h51KI mice were isolated for electrophysiological analysis. Briefly, soleus and EDL muscles were surgically isolated from 4-week-old Δ50;h51KI mice, mounted on Grass FT03.C force transducers, bathed in physiological salt solution at 37°C, and gassed continuously with 95% O_2 and 5% CO_2. After calibration, muscles were adjusted to an initial length, at which the passive force was 0.5 g, and then stimulated with two platinum wire electrodes to establish optimal length (Lo) for obtaining maximal isometric tetanic tension, step by step following the protocol (at 150 Hz for 2 s). Specific force (mN/mm^2) was calculated by normalizing contraction force to muscle cross-sectional area.

Statistics

All data are shown as means ± SEM. Unpaired two-tailed Student's t tests were performed to analyze Figures 1G and S2E. One-way analysis of variance (ANOVA) with post-hoc Tukey's multiple comparisons test was performed to analyze Figures 5A–5D and S8. Two-way ANOVA with post-hoc Tukey's multiple comparisons test was performed to analyze Figure S4. $p < 0.05$ was considered statistically significant. Data analyses were performed with GraphPad Prism Software.

Data and materials availability

All data needed to evaluate the conclusions in the paper are present in the paper and/or the supplemental information. Additional data related to this paper may be requested from the authors.

SUPPLEMENTAL INFORMATION

Supplemental information can be found online at https://doi.org/10.1016/j.omtn.2022.07.024.

ACKNOWLEDGMENTS

We thank J. Cabrera for graphics; Y.Z. and the Boston Children's Hospital Viral Core for AAV production; J. Kim and L. Xu for deep sequencing analysis; the Metabolic Phenotyping Core for serum CK analysis; the Sanger Sequencing Core and the Next Generation Sequencing Core for sequencing services; the Flow Cytometry Core for cell sorting; and the Histology Core for H&E staining. We are grateful to S. Hauschka (University of Washington) for providing the muscle-specific CK8e promoter. This work was supported by the NIH (grant R01 HL130253), the Senator Paul D. Wellstone Muscular Dystrophy Specialized Research Center (grant P50 HD 087351), and the Robert A. Welch Foundation (grant 1-0025 to E.N.O.).

AUTHOR CONTRIBUTIONS

Y.Z., R.B.-D., and E.N.O. wrote and edited the manuscript. Y.Z. designed the experiments, screened sgRNAs, cloned AAV constructs, and performed iPSC culture, animal studies, tissue cryosectioning, imaging, and data analysis. H.L. performed sgRNA screening, indel analysis, genomic PCR, RT-PCR, and data analysis. T.N. performed iPSC culture, western blot, and immunocytochemistry. J.R.M. performed the zygote injection to generate the Δ50;h51KI mice. J.H. performed the muscle electrophysiology analysis. E.S.-O. performed

immunohistochemistry, western blot, and imaging. P.P.A.M. provided oversight of the electrophysiology analysis.

DECLARATION OF INTERESTS

E.N.O. is a consultant for Vertex Pharmaceuticals. The other authors declare that they have no competing interests.

REFERENCES

1. Hoffman, E.P., Brown, R.H., Jr., and Kunkel, L.M. (1987). Dystrophin: the protein product of the Duchenne muscular dystrophy locus. Cell *51*, 919–928.
2. Koenig, M., Hoffman, E.P., Bertelson, C.J., Monaco, A.P., Feener, C., and Kunkel, L.M. (1987). Complete cloning of the Duchenne muscular dystrophy (DMD) cDNA and preliminary genomic organization of the DMD gene in normal and affected individuals. Cell *50*, 509–517.
3. Gao, Q.Q., and McNally, E.M. (2015). The dystrophin complex: structure, function, and implications for therapy. Compr. Physiol. *5*, 1223–1239. https://doi.org/10.1002/cphy.c140048.
4. Guiraud, S., Aartsma-Rus, A., Vieira, N.M., Davies, K.E., van Ommen, G.J.B., and Kunkel, L.M. (2015). The pathogenesis and therapy of muscular dystrophies. Annu. Rev. Genomics Hum. Genet. *16*, 281–308. https://doi.org/10.1146/annurev-genom-090314-025003.
5. Zhang, Y., Long, C., Bassel-Duby, R., and Olson, E.N. (2018). Myoediting: toward prevention of muscular dystrophy by therapeutic genome editing. Physiol. Rev. *98*, 1205–1240. https://doi.org/10.1152/physrev.00046.2017.
6. Zhang, Y., Nishiyama, T., Olson, E.N., and Bassel-Duby, R. (2021). CRISPR/Cas correction of muscular dystrophies. Exp. Cell Res. *408*, 112844. https://doi.org/10.1016/j.yexcr.2021.112844.
7. Chemello, F., Bassel-Duby, R., and Olson, E.N. (2020). Correction of muscular dystrophies by CRISPR gene editing. J. Clin. Invest. *130*, 2766–2776. https://doi.org/10.1172/JCI136873.
8. Bengtsson, N.E., Hall, J.K., Odom, G.L., Phelps, M.P., Andrus, C.R., Hawkins, R.D., Hauschka, S.D., Chamberlain, J.R., and Chamberlain, J.S. (2017). Muscle-specific CRISPR/Cas9 dystrophin gene editing ameliorates pathophysiology in a mouse model for Duchenne muscular dystrophy. Nat. Commun. *8*, 14454. https://doi.org/10.1038/ncomms14454.
9. Long, C., Amoasii, L., Mireault, A.A., McAnally, J.R., Li, H., Sanchez-Ortiz, E., Bhattacharyya, S., Shelton, J.M., Bassel-Duby, R., and Olson, E.N. (2016). Postnatal genome editing partially restores dystrophin expression in a mouse model of muscular dystrophy. Science *351*, 400–403. https://doi.org/10.1126/science.aad5725.
10. Nelson, C.E., Hakim, C.H., Ousterout, D.G., Thakore, P.I., Moreb, E.A., Castellanos Rivera, R.M., Madhavan, S., Pan, X., Ran, F.A., Yan, W.X., et al. (2016). In vivo genome editing improves muscle function in a mouse model of Duchenne muscular dystrophy. Science *351*, 403–407. https://doi.org/10.1126/science.aad5143.
11. Tabebordbar, M., Zhu, K., Cheng, J.K.W., Chew, W.L., Widrick, J.J., Yan, W.X., Maesner, C., Wu, E.Y., Xiao, R., Ran, F.A., et al. (2016). In vivo gene editing in dystrophic mouse muscle and muscle stem cells. Science *351*, 407–411. https://doi.org/10.1126/science.aad5177.
12. Bladen, C.L., Salgado, D., Monges, S., Foncuberta, M.E., Kekou, K., Kosma, K., Dawkins, H., Lamont, L., Roy, A.J., Chamova, T., et al. (2015). The TREAT-NMD DMD Global Database: analysis of more than 7, 000 Duchenne muscular dystrophy mutations. Hum. Mutat. *36*, 395–402. https://doi.org/10.1002/humu.22758.
13. Amoasii, L., Long, C., Li, H., Mireault, A.A., Shelton, J.M., Sanchez-Ortiz, E., McAnally, J.R., Bhattacharyya, S., Schmidt, F., Grimm, D., et al. (2017). Single-cut genome editing restores dystrophin expression in a new mouse model of muscular dystrophy. Sci. Transl. Med. *9*, eaan8081. https://doi.org/10.1126/scitranslmed.aan8081.
14. Min, Y.L., Chemello, F., Li, H., Rodriguez-Caycedo, C., Sanchez-Ortiz, E., Mireault, A.A., McAnally, J.R., Shelton, J.M., Zhang, Y., Bassel-Duby, R., and Olson, E.N. (2020). Correction of three prominent mutations in mouse and human models of Duchenne muscular dystrophy by single-cut genome editing. Mol. Ther. *28*, 2044–2055. https://doi.org/10.1016/j.ymthe.2020.05.024.
15. Min, Y.L., Li, H., Rodriguez-Caycedo, C., Mireault, A.A., Huang, J., Shelton, J.M., McAnally, J.R., Amoasii, L., Mammen, P.P.A., Bassel-Duby, R., and Olson, E.N. (2019). CRISPR-Cas9 corrects Duchenne muscular dystrophy exon 44 deletion mutations in mice and human cells. Sci. Adv. *5*, eaav4324. https://doi.org/10.1126/sciadv.aav4324.
16. Chemello, F., Wang, Z., Li, H., McAnally, J.R., Liu, N., Bassel-Duby, R., and Olson, E.N. (2020). Degenerative and regenerative pathways underlying Duchenne muscular dystrophy revealed by single-nucleus RNA sequencing. Proc. Natl. Acad. Sci. USA *117*, 29691–29701. https://doi.org/10.1073/pnas.2018391117.
17. Kyrychenko, V., Kyrychenko, S., Tiburcy, M., Shelton, J.M., Long, C., Schneider, J.W., Zimmermann, W.H., Bassel-Duby, R., and Olson, E.N. (2017). Functional correction of dystrophin actin binding domain mutations by genome editing. JCI Insight *2*, 95918. https://doi.org/10.1172/jci.insight.95918.
18. Amoasii, L., Li, H., Zhang, Y., Min, Y.L., Sanchez-Ortiz, E., Shelton, J.M., Long, C., Mireault, A.A., Bhattacharyya, S., McAnally, J.R., et al. (2019). In vivo non-invasive monitoring of dystrophin correction in a new Duchenne muscular dystrophy reporter mouse. Nat. Commun. *10*, 4537. https://doi.org/10.1038/s41467-019-12335-x.
19. Zhang, Y., Li, H., Min, Y.L., Sanchez-Ortiz, E., Huang, J., Mireault, A.A., Shelton, J.M., Kim, J., Mammen, P.P.A., Bassel-Duby, R., and Olson, E.N. (2020). Enhanced CRISPR-Cas9 correction of Duchenne muscular dystrophy in mice by a self-complementary AAV delivery system. Sci. Adv. *6*, eaay6812. https://doi.org/10.1126/sciadv.aay6812.
20. Zhang, Y., Nishiyama, T., Li, H., Huang, J., Atmanli, A., Sanchez-Ortiz, E., Wang, Z., Mireault, A.A., Mammen, P.P.A., Bassel-Duby, R., and Olson, E.N. (2021). A consolidated AAV system for single-cut CRISPR correction of a common Duchenne muscular dystrophy mutation. Mol. Ther. Methods Clin. Dev. *22*, 122–132. https://doi.org/10.1016/j.omtm.2021.05.014.
21. Amoasii, L., Hildyard, J.C.W., Li, H., Sanchez-Ortiz, E., Mireault, A., Caballero, D., Harron, R., Stathopoulou, T.R., Massey, C., Shelton, J.M., et al. (2018). Gene editing restores dystrophin expression in a canine model of Duchenne muscular dystrophy. Science *362*, 86–91. https://doi.org/10.1126/science.aau1549.
22. Aartsma-Rus, A., Fokkema, I., Verschuuren, J., Ginjaar, I., van Deutekom, J., van Ommen, G.J., and den Dunnen, J.T. (2009). Theoretic applicability of antisense-mediated exon skipping for Duchenne muscular dystrophy mutations. Hum. Mutat. *30*, 293–299. https://doi.org/10.1002/humu.20918.
23. Kleinstiver, B.P., Pattanayak, V., Prew, M.S., Tsai, S.Q., Nguyen, N.T., Zheng, Z., and Joung, J.K. (2016). High-fidelity CRISPR-Cas9 nucleases with no detectable genome-wide off-target effects. Nature *529*, 490–495. https://doi.org/10.1038/nature16526.
24. Nishimasu, H., Shi, X., Ishiguro, S., Gao, L., Hirano, S., Okazaki, S., Noda, T., Abudayyeh, O.O., Gootenberg, J.S., Mori, H., et al. (2018). Engineered CRISPR-Cas9 nuclease with expanded targeting space. Science *361*, 1259–1262. https://doi.org/10.1126/science.aas9129.
25. Himeda, C.L., Chen, X., and Hauschka, S.D. (2011). Design and testing of regulatory cassettes for optimal activity in skeletal and cardiac muscles. Methods Mol. Biol. *709*, 3–19. https://doi.org/10.1007/978-1-61737-982-6_1.
26. Hakim, C.H., Wasala, N.B., Nelson, C.E., Wasala, L.P., Yue, Y., Louderman, J.A., Lessa, T.B., Dai, A., Zhang, K., Jenkins, G.J., et al. (2018). AAV CRISPR editing rescues cardiac and muscle function for 18 months in dystrophic mice. JCI Insight *3*, 124297. https://doi.org/10.1172/jci.insight.124297.
27. Veltrop, M., van Vliet, L., Hulsker, M., Claassens, J., Brouwers, C., Breukel, C., van der Kaa, J., Linssen, M.M., den Dunnen, J.T., Verbeek, S., et al. (2018). A dystrophic Duchenne mouse model for testing human antisense oligonucleotides. PLoS One *13*, e0193289. https://doi.org/10.1371/journal.pone.0193289.
28. Young, C.S., Mokhonova, E., Quinonez, M., Pyle, A.D., and Spencer, M.J. (2017). Creation of a novel humanized dystrophic mouse model of Duchenne muscular dystrophy and application of a CRISPR/Cas9 gene editing therapy. J. Neuromuscul. Dis. *4*, 139–145. https://doi.org/10.3233/JND-170218.
29. Yavas, A., Weij, R., van Putten, M., Kourkouta, E., Beekman, C., Puoliväli, J., Bragge, T., Ahtoniemi, T., Knijnenburg, J., Hoogenboom, M.E., et al. (2020). Detailed genetic and functional analysis of the hDMDdel52/mdx mouse model. PLoS One *15*, e0244215. https://doi.org/10.1371/journal.pone.0244215.

30. Jinek, M., Chylinski, K., Fonfara, I., Hauer, M., Doudna, J.A., and Charpentier, E. (2012). A programmable dual-RNA-guided DNA endonuclease in adaptive bacterial immunity. Science *337*, 816–821. https://doi.org/10.1126/science.1225829.

31. Cameron, P., Fuller, C.K., Donohoue, P.D., Jones, B.N., Thompson, M.S., Carter, M.M., Gradia, S., Vidal, B., Garner, E., Slorach, E.M., et al. (2017). Mapping the genomic landscape of CRISPR-Cas9 cleavage. Nat. Methods *14*, 600–606. https://doi.org/10.1038/nmeth.4284.

32. Tsai, S.Q., Zheng, Z., Nguyen, N.T., Liebers, M., Topkar, V.V., Thapar, V., Wyvekens, N., Khayter, C., Iafrate, A.J., Le, L.P., et al. (2015). GUIDE-seq enables genome-wide profiling of off-target cleavage by CRISPR-Cas nucleases. Nat. Biotechnol. *33*, 187–197. https://doi.org/10.1038/nbt.3117.

33. Hakim, C.H., Kumar, S.R.P., Pérez-López, D.O., Wasala, N.B., Zhang, D., Yue, Y., Teixeira, J., Pan, X., Zhang, K., Million, E.D., et al. (2021). Cas9-specific immune responses compromise local and systemic AAV CRISPR therapy in multiple dystrophic canine models. Nat. Commun. *12*, 6769. https://doi.org/10.1038/s41467-021-26830-7.

34. Charlesworth, C.T., Deshpande, P.S., Dever, D.P., Camarena, J., Lemgart, V.T., Cromer, M.K., Vakulskas, C.A., Collingwood, M.A., Zhang, L., Bode, N.M., et al. (2019). Identification of preexisting adaptive immunity to Cas9 proteins in humans. Nat. Med. *25*, 249–254. https://doi.org/10.1038/s41591-018-0326-x.

35. Wagner, D.L., Peter, L., and Schmueck-Henneresse, M. (2021). Cas9-directed immune tolerance in humans-a model to evaluate regulatory T cells in gene therapy? Gene Ther. *28*, 549–559. https://doi.org/10.1038/s41434-021-00232-2.

36. Dowling, J.J. (2022). CRISPR editing as a therapeutic strategy for Duchenne muscular dystrophy-anti-Cas9 immune response casts its shadow over safety and efficacy. Gene Ther. https://doi.org/10.1038/s41434-022-00323-8.

37. Hinderer, C., Katz, N., Buza, E.L., Dyer, C., Goode, T., Bell, P., Richman, L.K., and Wilson, J.M. (2018). Severe toxicity in nonhuman primates and piglets following high-dose intravenous administration of an adeno-associated virus vector expressing human SMN. Hum. Gene Ther. *29*, 285–298. https://doi.org/10.1089/hum.2018.015.

38. Kornegay, J.N., Li, J., Bogan, J.R., Bogan, D.J., Chen, C., Zheng, H., Wang, B., Qiao, C., Howard, J.F., Jr., and Xiao, X. (2010). Widespread muscle expression of an AAV9 human mini-dystrophin vector after intravenous injection in neonatal dystrophin-deficient dogs. Mol. Ther. *18*, 1501–1508. https://doi.org/10.1038/mt.2010.94.

39. Tabebordbar, M., Lagerborg, K.A., Stanton, A., King, E.M., Ye, S., Tellez, L., Krunnfusz, A., Tavakoli, S., Widrick, J.J., Messemer, K.A., et al. (2021). Directed evolution of a family of AAV capsid variants enabling potent muscle-directed gene delivery across species. Cell *184*, 4919–4938.e22. https://doi.org/10.1016/j.cell.2021.08.028.

40. Weinmann, J., Weis, S., Sippel, J., Tulalamba, W., Remes, A., El Andari, J., Herrmann, A.K., Pham, Q.H., Borowski, C., Hille, S., et al. (2020). Identification of a myotropic AAV by massively parallel in vivo evaluation of barcoded capsid variants. Nat. Commun. *11*, 5432. https://doi.org/10.1038/s41467-020-19230-w.

41. Hu, Z., Wang, S., Zhang, C., Gao, N., Li, M., Wang, D., Wang, D., Liu, D., Liu, H., Ong, S.G., et al. (2020). A compact Cas9 ortholog from Staphylococcus Auricularis (SauriCas9) expands the DNA targeting scope. PLoS Biol. *18*, e3000686. https://doi.org/10.1371/journal.pbio.3000686.

42. Hu, Z., Zhang, C., Wang, S., Gao, S., Wei, J., Li, M., Hou, L., Mao, H., Wei, Y., Qi, T., et al. (2021). Discovery and engineering of small SlugCas9 with broad targeting range and high specificity and activity. Nucleic Acids Res. *49*, 4008–4019. https://doi.org/10.1093/nar/gkab148.

43. Hoffman, E.P., Kunkel, L.M., Angelini, C., Clarke, A., Johnson, M., and Harris, J.B. (1989). Improved diagnosis of Becker muscular dystrophy by dystrophin testing. Neurology *39*, 1011–1017. https://doi.org/10.1212/wnl.39.8.1011.

44. Brinkman, E.K., Chen, T., Amendola, M., and van Steensel, B. (2014). Easy quantitative assessment of genome editing by sequence trace decomposition. Nucleic Acids Res. *42*, e168. https://doi.org/10.1093/nar/gku936.

45. Zhang, Y., Long, C., Li, H., McAnally, J.R., Baskin, K.K., Shelton, J.M., Bassel-Duby, R., and Olson, E.N. (2017). CRISPR-Cpf1 correction of muscular dystrophy mutations in human cardiomyocytes and mice. Sci. Adv. *3*, e1602814. https://doi.org/10.1126/sciadv.1602814.